Available online www.jocpr.com

Journal of Chemical and Pharmaceutical Research, 2014, 6(9):469-487

Research Article

ISSN : 0975-7384
CODEN(USA) : JCPRC5

Effects of hydrolyzation, aging time and temperature on rheology of sols and effects of aging and sintering temperatures on structural and thermal properties of calcium phosphate powders

Ravinder Pal Singh* and Uma Batra

Department of Materials and Metallurgical Engineering, PEC University of Technology, Chandigarh, India

---

ABSTRACT

Among the various process parameters of sol-gel technique, aging time and temperature play decisive roles and affect the properties of precursors, sol and synthesized product to a large extent. A detailed analysis including various rheological properties of Calcium and Phosphorous based precursors at ambient temperature and Calcium Phosphate sol at 5°C and 25°C have been carried out in the present paper. Comprehensive effects of aging temperatures on structural and thermal properties of Calcium Phosphate based powders have also been characterized by using X-Ray Diffraction, Fourier Transform Infrared, Thermogravimetric/Differential Scanning Calorimetery, Transmission Electron Microscopy and Scanning Electron cum Energy Dispersive Microscopy. The hydrolysis of precursors was found to have profound effect on their rheology. pH and density of CaP sols were found to be independent on aging time and temperature. Formation of calcium deficient HAP, HAP, β-TCP and α-TCP in CaP powders were revealed from XRD patterns. FTIR results showed the presence of HPO_4^{-2} and PO_4 ions for all sintering temperatures in both the aged powders. SEM showed the powders have granular, irregular, loose but smooth mixture of solid rod and plate like nano regime particles. Average particle size ranged from 100-150 µm and 105-180 µm for powders aged at 25°C and 5°C respectively. EDX presented the results in line with XRD detections. Hexagonal shape of crystals having sharp edges of both the powders was observed from TEM micrographs. Larger crystals were observed in case of 25°C aged powders.

Keywords: Aging Time, Aging Temperature, HAP, CaP, Viscosity, XRD, FTIR.

INTRODUCTION

Bioactive and bioresorbable phases of CaP powders are materials of choice for innumerable bone-tissue engineering applications [1,2]. Among the various bioceramics; HAP and β-TCP are most widely used, because these promote osteogenesis and firm tight bonds with host bone tissues [3] although, the degradation rate of β-TCP is 10 times higher than that of HAP [4]. This resulted in the growing interest in developing HAP/ β-TCP Biphasic Calcium Phosphate (BCP) ceramics due to its controllable degradation rate and more effective bone regeneration ability [5].

Though innumerable processes have been used to synthesize BCP bioceramics, only a few techniques have been developed to synthesize nano-powders. Of these, sol-gel synthesis has recently attracted much attention [6,7] owing to its multiple advantages including molecular-level mixing of precursors [2] which is capable of improving chemical homogeneity [2,8,9] of the resulting product to a significant extent; reduced sintering temperature due to small particle size [8]; few equipments used; high output and easy operation process [10] in comparison to conventional methods such as solid state reactions [9,11], polymeric precursor route [12], wet precipitation method [9,13] and micro emulsion technique [14] etc. Furthermore, sol-gel process can produce fine-grain microstructures containing a mixture of nano-to-submicron apatitic crystals [7,15]. These crystals can be better accepted by host tissue [7,16]. Low temperature formation and fusion of the apatitic crystals has been the main contribution of the sol-gel process [7] and hence has been widely studied by many investigators [17-19]. The use of sol-gel process in

the biomedical area is recent. The first paper came out about 10 years ago, and the number of publications has increased noticeably during the last five years [20].

Sol-gel process usually comprises of five main steps: (1) hydrolysis and polycondensation, (2) gelation, (3) aging, (4) drying, (5) densification and crystallization [21]. Each of these stages and their respective process parameters affect the overall properties of precursors, sol and the resultant product to a large extent [22]. Extensive literature was reviewed to ascertain the effects of different sol-gel process parameters on the characteristics of CaP powders. Liu et al. [9] investigated the influence of hydrolysis of 'P' sol solution on the phase evolution of the resulting HAP and concluded that long-term hydrolysis is required for better evolution of apatitic phases in the absence of acid catalyst. Hydrolysis can be monitored by testing its pH value [23].

Masuda et al. [24] found that the determining factor for the composition of the resultant powder is solution pH [22]. Hsieh et al. [23] measured the pH value of precursors only before and after the aging period. pH values were not reported during aging. Liu et al. [9] measured the pH of TEP and CaP solutions up to 24 hours only.

Viscosity of precursors and final solutions was also not analyzed comprehensively which could have strengthened the understanding of controlling the films on substrates while coating. Very few papers are available which discuss the viscosity [25,26], but in a very little perspective.

Chai et al. [8] addressed the effect of aging time on the composition of coating and the time required for the solution before depositing monophasic coatings and concluded that the solution aging time of at least 01 day is essential to deposit monophasic HAP coatings. Similarly, Liu et al. [29] also indicated that a specific aging time period either at ambient or higher temperature is necessary to form a phase-pure apatite. Insufficient aging causes appearance of impurity phases, such as CaO or $CaCO_3$ [7]. Liu et al. [7] investigated the structural evolution during the transition of sol to gel, and to the final crystalline apatite at 45°C for time periods up to 120 minutes. Nissan et al. [22] expressed that aging of HAP solution between 6-8 days increased HAP formation and suggested that a critical factor in determining the composition of the final coating is the period between solution preparation and coating deposition (aging time). Gross et al. [27] also emphasized that the chemical phase purity of the powder and coating is dictated by the purity of precursor material and the aging time of solution.

Effect of heating on the production of uniform HAP powders and coatings were also investigated [27]. Hsieh et al. pointed out that the thermal treatment generally plays a very important role in the formation of the precursors because stoichiometry of calcined powders is correlated with molecular arrangement in which heating provides energy to arrange the precursors [23]. Hsieh et al. used the higher aging temperature ranges from 80-90°C in his study. The effect of reaction temperature (15-60°C) on the kinetics of HAP precipitation was also studied by Cui and co-authors [28] and reported that the HAP precipitation is highly temperature dependent and the nucleation rate is faster at higher temperature. Further, they also demonstrated that the temperature has a great influence on both the particle size and the morphology of the precipitated HAP or product [28].

Effects of sintering temperature and sintering time on the properties of synthetic bioceramics have been widely studied by numerous authors [30-32].

Keeping in mind the insufficient reporting of rheological properties of especially Ca and P based precursors during hydrolysis and their mixed sols during aging at various temperatures and times inspired the present authors to study them comprehensively. In addition, dearth of investigations comprehending the effects of aging temperature on structural, thermal and elemental characteristics of CaP powders became another objective of the present paper.

EXPERIMENTAL SECTION

2.1. Materials

CNT (Merck, 98% Pure) and TEP [Spectrochem, 98% Pure, Specific Gravity= 0.969 g/ml] were used as a Ca and P ion sources throughout the investigation. Double distilled water (DDH_2O) and ethanol [Merck, 99.9% pure] were used as solvents. Ammonium Hydroxide [25%, Merck] was used to increase the pH of CaP solution to improve its gelation.

Methodology for the synthesis of CaP based precursors, sols and powders has been explained in Figure 1.

2.2. Synthesis of CaP Precursors, Sols and Powders

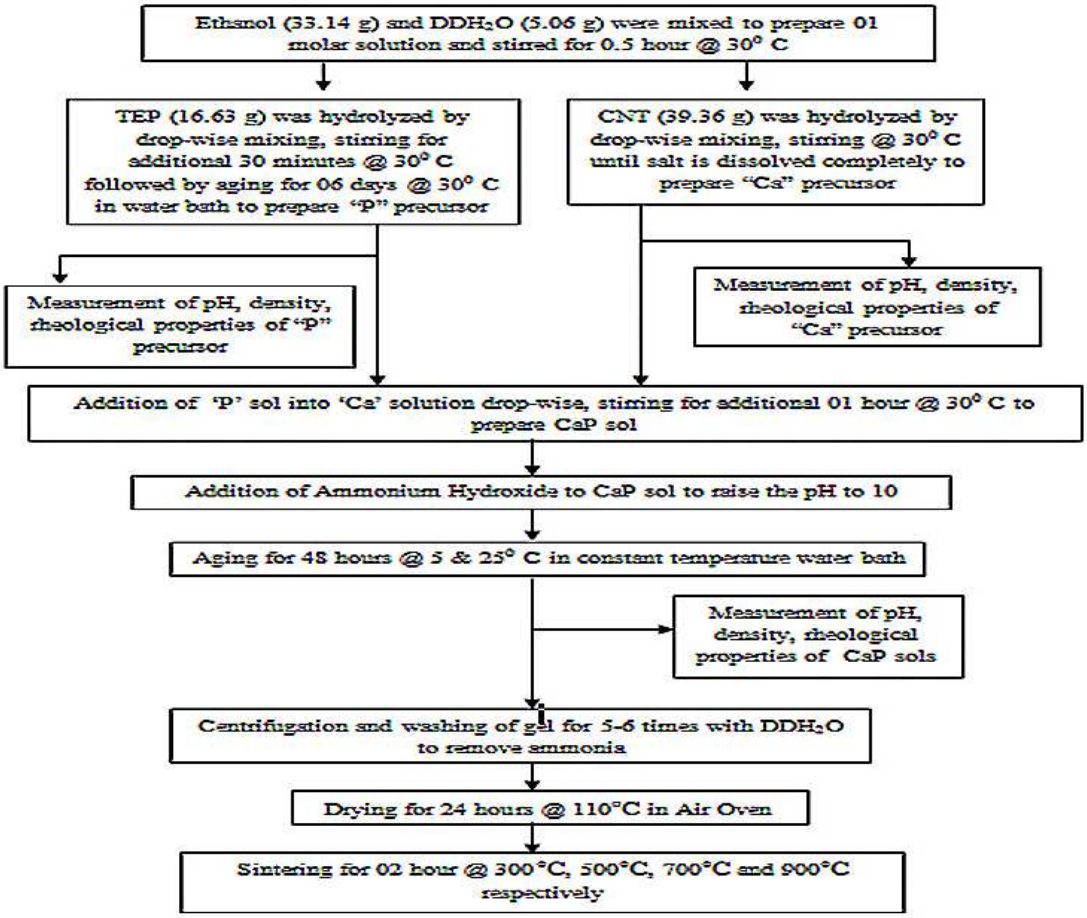

Figure 1. Synthesis Methodology

2.3. Sol Characterization

Digital pH meter (MAX, India) was used to measure the pH value of solutions. Digital weighing-cum-density meter (SI-234; Denver Instruments) was used to measure the density of solutions. A special attachment meant for measuring density of solutions was employed throughout.

Rheological properties viz. % torque, viscosity, shear stress and shear rate were analyzed using programmable Rheometer (Brookfield, DV-III Ultra). Special attachment UL adaptor along with spindle no- 87 were used to measure the rheological properties. % torque, viscosity, shear stress and shear rate of various solutions were measured.

2.4. Powder Characterization

X-Ray Diffraction (Philips X'Pert 1710) analysis was performed for all powders using CuKα radiation (λ= 1.54 Å, 2θ= 20° to 50°, step size 0.017°, time per step 20.03 s and scan speed 0.005°/s). Relative amount of different phases present were estimated on the basis of the peak intensity variation by means of external standard method. Both cell parameters, a and c has been calculated using the equation given below:

$$\frac{1}{d^2} = \frac{4}{3}\left\{\frac{h^2+hk+k^2}{a^2}\right\} + \frac{l^2}{c^2} \qquad \text{(Eq. 1)}$$

where d is the distance between adjacent planes in the set of Miller indices (h k l), the reference for HAP being JCPDS file no. 09-0432 (a=9.418 Å, b=9.418 Å, c=6.884 Å, space group p63/m), for β-TCP being JCPDS file no. 09-0169 (a=10.432 Å, b=10.432 Å, c=37.39 Å, space group R3c (167)) and for α-Tricalcium Phosphate (α-TCP) being JCPDS file no. 03-0681. Crystallite size was calculated using Scherrer's equation:

$$X_s = \frac{0.9\,\lambda}{\beta\, Cos\, \Theta} \qquad \text{(Eq. 2)}$$

Where X_s is the crystallite size in nanometer, λ is the wave length of x-ray beam, β is the broadening of diffraction line at half of its maximum intensity in radians, and θ is the Bragg's diffraction angle (°). The silicon standard was used to measure the instrument broadening to correct the value of β. The three diffraction peaks (0 0 2), (2 0 2) and (2 2 2) which are well separated or peaks having high intensities were chosen to calculate mean crystallite size of HAP lattice. For calculating domain sizes along the crystallographic axis c and a of HAP lattice, the diffraction peaks at 25.8° (2θ) corresponding to (0 0 2) and 32.9° (2θ) corresponding to (3 0 0) were considered.

The relative amounts of HAP and β-TCP in the synthesized powder were determined using external standard method as given in Eq. 3.

$$\frac{I_{\beta TCP(0210)}}{I_{HAP(211)}} = \frac{\text{Weight of } \beta-\text{TCP}}{\text{Weight of HAP}} \quad \text{(Eq. 3)}$$

Where $I_{\beta\text{-TCP }(0210)}$ is the intensity of β-TCP peak having (0 2 1 0) as (h k l) plane and I_{HAP} is the intensity of HAP peak having (2 1 1) as (h k l) plane respectively.

Calcium deficiency (x) of synthetic HAP powder was calculated by converting the weight ratio into molar ratio as follows:

$$\frac{Mol_{\beta TCP}}{Mol_{HAP}} = \frac{Wt_{\beta TCP}}{Wt_{HAP}} \text{ x } 3.23 \quad \text{(Eq. 4)}$$

$$\frac{Mol_{\beta TCP}}{Mol_{HAP}} = \frac{3x}{1-x} \quad \text{(Eq. 5)}$$

Where x is a calcium deficiency of synthesized powder.

Calcium to phosphorous (Ca/P) ratio was further calculated using Eq. 6 as follows:

$$\frac{Ca}{P} = \frac{10-x}{6} \quad \text{(Eq. 6)}$$

Infrared spectra (FTIR Perkin Elmer) were recorded in the region 500-4000 cm^{-1} using KBr pellets (1% wt/wt), with spectral resolution of 2 cm^{-1}, taking four scans for each sample.

Thermal behavior of as-synthesized gel was investigated using simultaneous Thermogravimetry and Differential Scanning Calorimetry (TGA/DSC, Perkin Elmer STA 6000), with an accuracy of ±0.1 µg in weight measurement and ±0.5 °C in temperature measurement. All the tests were performed in air environment under the following conditions: heating rate 10° C/min, peak temperature 1000°C, and air flow 20.0 mL/min.

Morphology of synthetic powders was observed using Scanning Electron Microscopy (SEM, JEOL); operated at a voltage of 30 kV. Presence of various constituent elements in powders was detected by Energy Dispersive Spectroscopy (EDX).

Shape and size of nano-crystals were observed using Transmission Electron Microscope (TEM) (Hitachi, 7500) with resolution of 0.2 nm, operated at an accelerating voltage of 80-100 kV. The powders were ultrasonically dispersed in ethanol to form a dilute suspension and then a drop of suspension was dropped on carbon-coated copper grid of 300 mesh for observation.

RESULTS AND DISCUSSION

3.1. Selection of TEP as Phosphorous Precursor and its Hydrolysis

CNT and TEP were chosen as Ca and P reagents in the present study. TEP was so selected, because it was reported that out of trialed phosphoric acid, phosphorous pentaoxide refluxed with 1-proponal and TEP as phosphorous precursors; an aqueous solution of latter is the only suitable phosphorous candidate [22]. Being an alkoxide, it's easy to prepare HAP or other allied phases by using TEP as a phosphorous reagent [9,32]. In addition, it's easy to hydrolyze TEP rapidly, as opposed to trialkyl phosphate precursors [9].

Non aqueous solvents are frequently employed for the dilution of TEP, together with a small amount of water for hydrolysis [9]. Water can be mixed with the ethanol solution due to the reason that polymerization reaction usually accompanied by hydrolysis [9]. TEP can be hydrolyzed in the presence of water or air moisture to form diethyl

phosphorous ester [33]. Therefore, a mixture of ethanol and water was prepared to dissolve into TEP in the present investigation.

In conjunction with the previous experimental observations, TEP remained immiscible with the water and formed emulsion phase after immediate mixing with water.

$$P(OC_2H_5)_3 + H_2O \rightarrow HPO(OC_2H_5) + C_2H_5OH \quad (7)$$

Masuda et al. [33] indicated that reaction (7) proceeds exceedingly slowly, for example 10 or more hours are required to complete. In the present study, this emulsion mixture turned into a clean solution along with the disappearance of phosphite odor only after 144 hours of hydrolysis (Figure 4), indicating completion of its hydrolysis. A continuous decrease in pH of TEP solution was detected for 144 hours (Figure 4) suggesting extended progress of hydrolysis, by the release of proton according to reaction 8. This strongly suggests that an extended hydrolysis of the diethyl phosphorous esters may undergo, where more –OR groups were replaced by –OH groups in reaction 9.

$$(CH_3OH)3P: + H^+ \leftrightarrow (CH_3OH)3P^+H$$
$$(CH_3OH)3P^+H + H_2O \rightarrow (CH_3O)2\,P(H) \quad (8)$$

$$= O{+}CH_3OH + H^+$$
$$HPO(OC_2H_5)2 + H_2O \rightarrow HPO(OC_2H_5)2 - x(OH)x + xC_2H_5OH \quad (9)$$

Sufficient hydrolysis causes the formation of more free solvents (i.e. C_2H_5OH in reaction 9) and is expected to remove easily on further treatments [9].

3.2. Effect of Hydrolysation Time on Rheological Properties of Precursors

Rheological properties of CNT and TEP solutions were measured [(at 20, 40, 70, 100, 140, 200 and 240 RPMs at ambient temperature (30°C)) during their hydrolysis up to 06 days (144 hours)]. Effect of hydrolysis on pH, density and rheological properties of CNT and TEP precursors can be comprehensively studied from Figures 2-5 respectively.

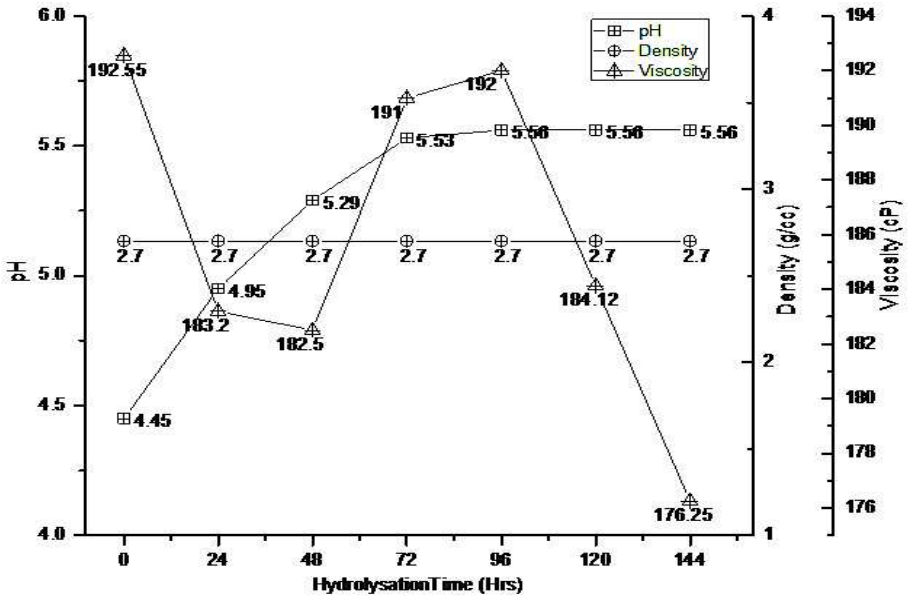

Figure 2. pH, Density and Viscosity of CNT Precursor at 30° C

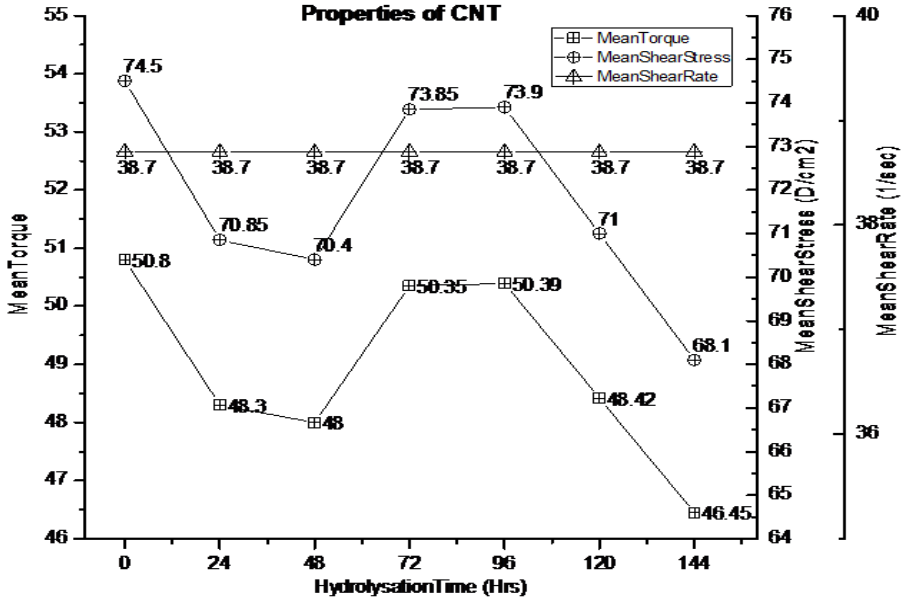

Figure 3. Mean Torque, Mean Shear Stress and Mean Shear Rate of CNT Precursor at 30° C

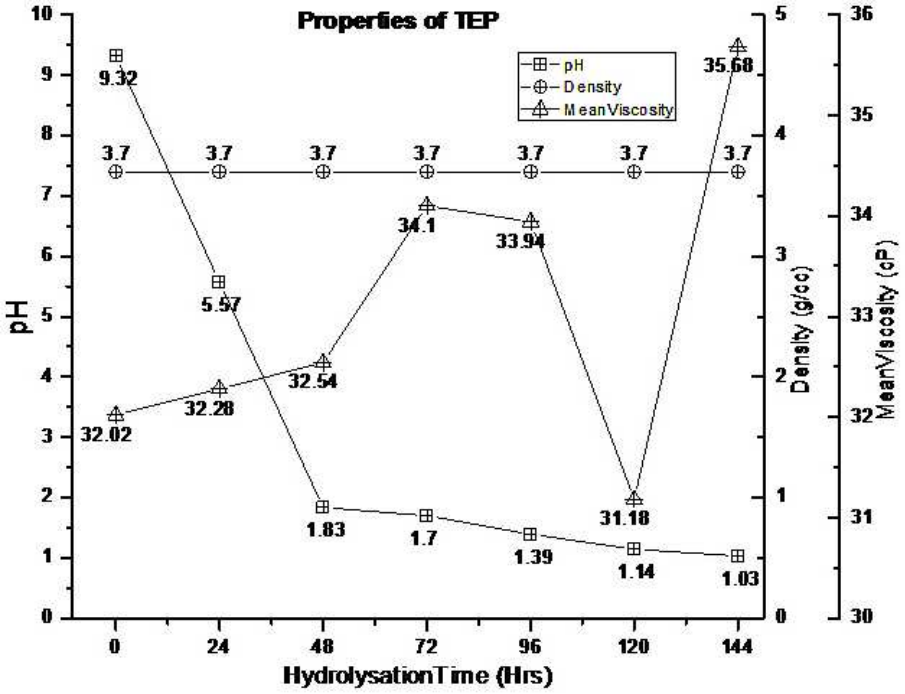

Figure 4. pH, Density and Viscosity of TEP Precursor at 30° C

Opposite behavior was observed in the rate of change of pH of CNT and TEP precursors as indicated in Figure 2 and Figure 4 respectively. pH of CNT precursor was found to increase, whereas it decreased continuously in case of TEP solution. Change in pH of TEP was continued for 144 hours (06 days), which supports the requirement of its hydrolysis for such a long time. After 144 hours, pH of TEP precursor came to stand still and was observed to be highly reactive (1.03) in nature. It is believed that incorporation of more acidic phosphate ions, such as HPO_4^{2-}, rather than more basic group PO_4^{3-}, into the resulting gel structure is more favorable [9]. On the other hand, pH gradient of CNT precursor was noticed to be negligible after 72 hours (03 days).

In light of uncertain behavior of rate of change of viscosity of both the CNT and TEP precursors, CNT precursor was noticed to be 05 times more viscous than TEP precursor corresponding to 144 hours at ambient temperature as enumerated in Figure 2 and Figure 4.

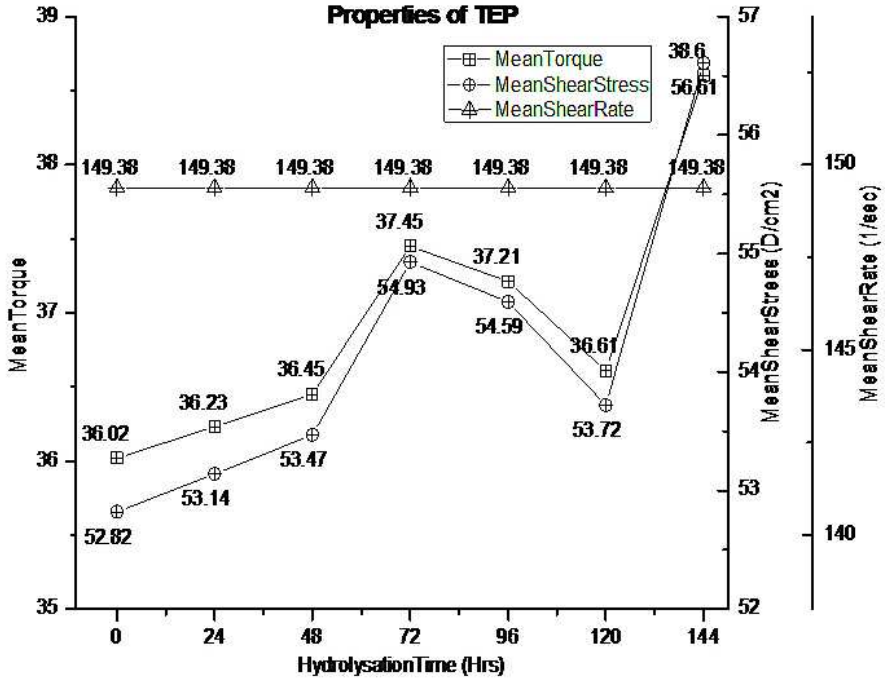

Figure 5. Mean Torque, Mean Shear Stress and Mean Shear Rate of TEP Precursor at 30° C

Density and mean shear rate of CNT and TEP precursors remained constant throughout all hydrolysation time periods as shown in Figure 2-5 respectively which indicate their independence on hydrolysation time.

Rate of change of % torque and shear stress of CNT and TEP precursors were ascertained to be directly proportional to each other as shown in Figure 3 and Figure 5 respectively. Ratio of shear stress to shear strain further validates the non-Newtonian and Newtonian nature of CNT and TEP solutions respectively.

3.3. CaP Sols and Their Properties

Following mixing of Ca and P precursors, hydrolyzed phosphite has been believed to interact with Ca ions in aqueous solution through a condensation polymerization reaction to form a Ca-P intermediate,

$$2\mathrm{HPO(OC_2H_5)2} - \mathrm{x(OH)x} + \mathrm{Ca} + + \rightarrow \mathrm{CaP\ intermediate} + 2\mathrm{H} + \qquad (10)$$

Neither precipitates nor solid like gel were ever observed for the prepared CaP sol even upon 07 days of aging. This may account for the partial charge model proposed by Livage et al. [35,36], where the degree of polymerization described in equation (10) must be low, resulting in oligomeric derivatives dispersed in solution, rather than a 3D network structure.

Condensation between hydrolyzed phosphite molecules to form oligomeric derivatives such as

$$2\mathrm{HPO(OC_2H_5)2} - \mathrm{x(OH)x} \rightarrow \mathrm{(OC_2H_5)2 - x\,O(H)P - O - P(H)O(OC_2\,H_5)2 - x} + 2\mathrm{H_2O} \qquad (11)$$

The oligomeric derivatives further hydrolyze (reaction 12) and reacts with Ca to form CaP derivatives, reaction 13:

$$\mathrm{(OC_2H_5)2 - x\,O(H)P - O - P(H)O(OC_2\,H_5)2 - x} + 2\mathrm{H_2O} \rightarrow \mathrm{(OC_2H_5)2 - y(OH)y(H)OP - O - P(H)O(OC_2\,H_5)2 - y(OH)y} + 2(\mathrm{x-y})\mathrm{C_2H_5OH} \qquad (12)$$

$$\mathrm{(OC_2H_5)2 - y(OH)y(H)OP - O - P(H)O(OC_2\,H_5)2 - y(OH)y\ + Ca-} \rightarrow \mathrm{Ca - O - (OC_2\,H_5)2 - y\ (H)OP - O - P(H)O(OC_2H_5)2 - y - O - Ca} + 2\mathrm{H} + + \mathrm{H_2O} \qquad (13)$$

Although above equations are of simplified and somewhat speculative chemical paths, these do propose the possibility for the formation of the CaP derivatives with lower Ca/P ratio than stoichiometry [9].

Therefore due to non-precipitation even after aging for many days, ammonium hydroxide was chosen to add into prepare CaP sol to raise its pH to 10, in order to increase its gelation. 10 pH was sol selected as it has been reported

that at pH values above 9, the most stable CaP phase in aqueous solution is HAP [39]. The liberation of proton in reaction (10) can be monitored by the change of solution pH as shown in Figure 6 and Figure 8, where the solution pH remained almost constant as a function of aging time for over a period of 48 hours. This also indicates a slow reaction between hydrolyzed phosphite and Ca ions.

3.4. Effect of Aging Time and Temperature on Rheological Properties of CaP Sols

After the addition of ammonium hydroxide in the mixture of 'Ca' and 'P' precursors, rate of change of pH, density and all rheological properties of resultant CaP solutions at controlled temperatures of 25℃ and 5℃ were measured and have been shown in Figures 6-9 respectively.

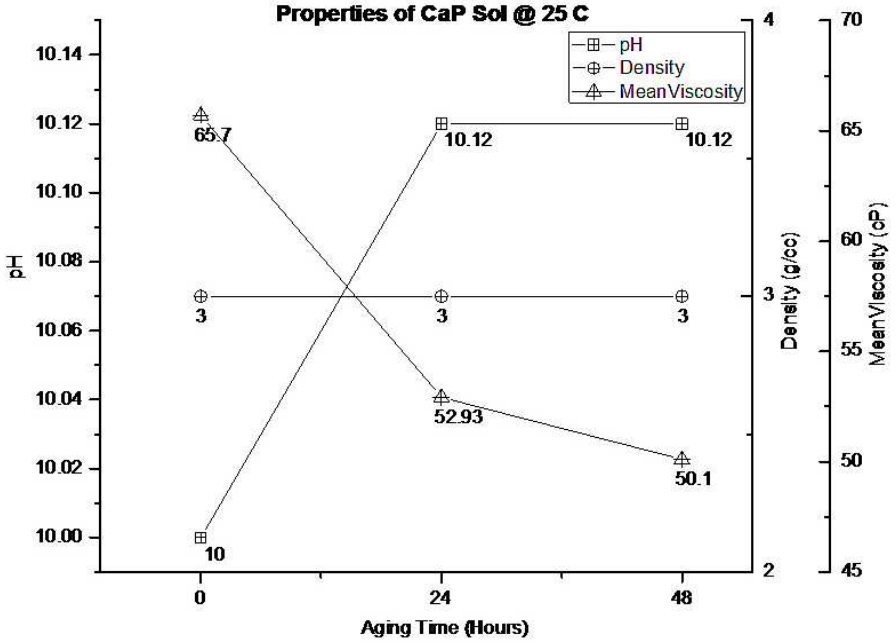

Figure 6. pH, Density and Viscosity of CaP Sol Aged at 25℃

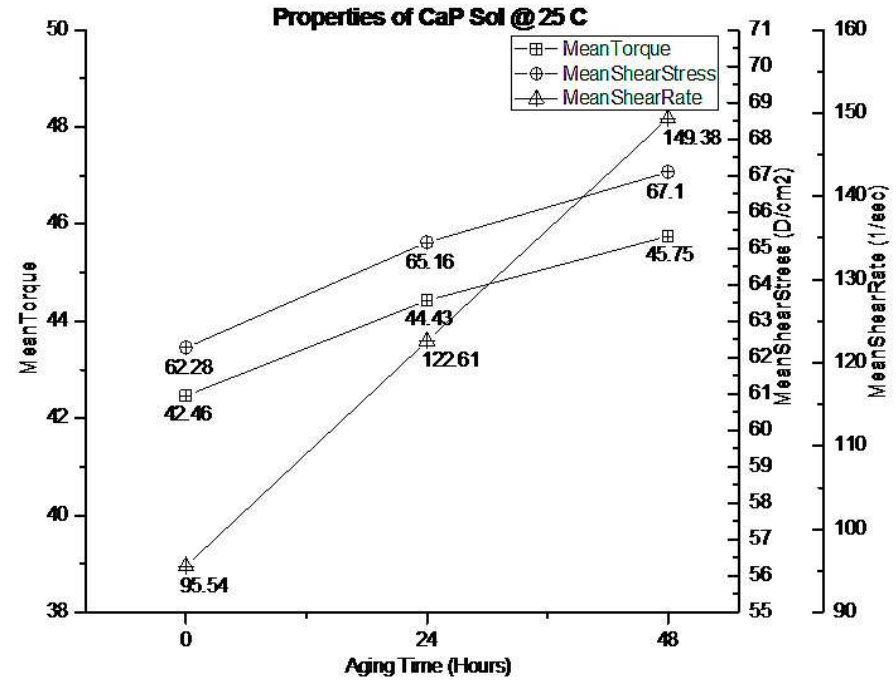

Figure 7. Various Rheological Properties of CaP Sol Aged at 25℃

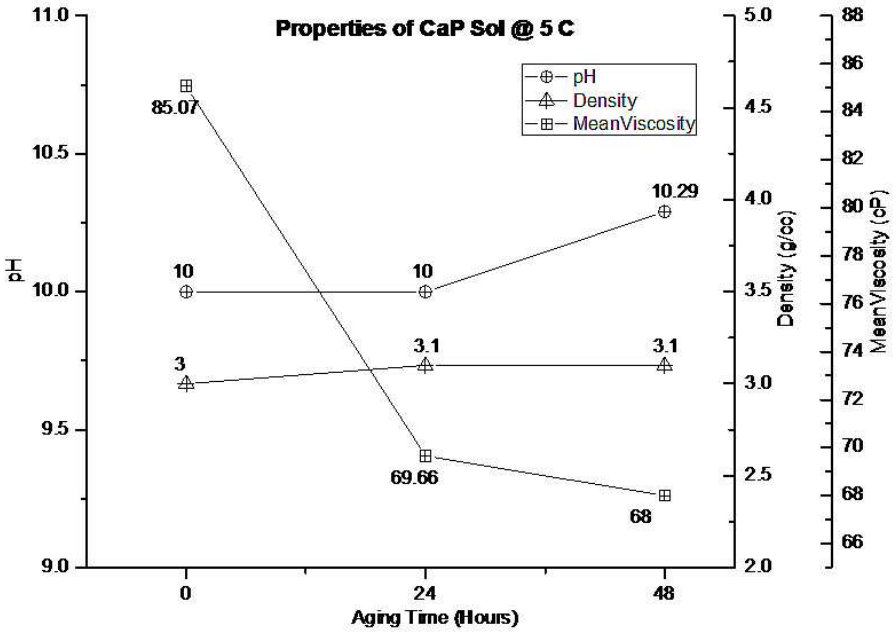

Figure 8. pH, Density and Viscosity of CaP Sol Aged at 5℃

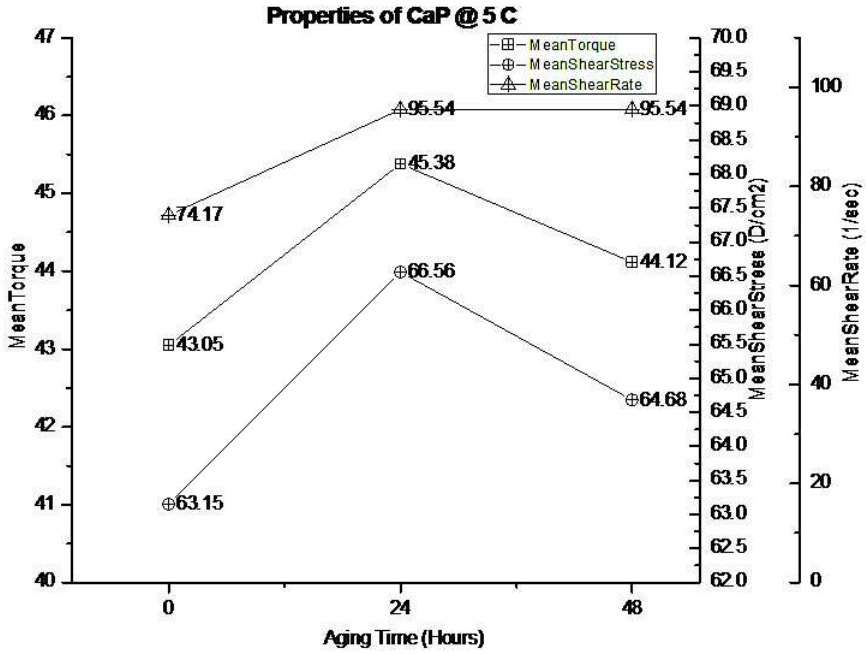

Figure 9. Various Rheological Properties of CaP Sol Aged at 5℃

Magnitude and rate of change of various properties of CaP solutions at different aging temperatures can be comprehensively studied from Figures 6-9 respectively. pH and density of resultant CaP were found to be independent of aging time and temperature as shown in Figure 6 and Figure 8 respectively. Density of solutions at both aging temperatures was found to be very near to each other as well as the theoretical value of HAP powder i.e. 3.18 g/cc, irrespective of different aging times.

CaP sol aged at 5℃ was found to be more viscous than the other sol aged at 25℃ during all aging times. On the other hand, a similar trend of decrease of viscosity was observed over the increasing aging time at both the aging temperatures.

Both the CaP precursors aged at different controlled temperatures were behaved as Non-Newtonian fluids, as the ratio of their mean shear stress to mean shear rate was not constant. Directly proportional relation between mean shear stress and mean %torque was observed in both the resultant solutions, notwithstanding any effect of temperature on them.

pH of both the CaP sols was remained almost constant with negligible change up to 48 hours of aging which indicates the absence of hydrolysis of TEP in the CaP mixture. It further supports the need of complete hydrolysis of TEP as a single precursor. That's why; hydrolysis of TEP was monitored and carried out for 144 hours in the present study. Highly hydrolyzed phosphorous ion precursor was expected to react with Ca ions present in the mixture easily and fastly to form a desirable complex.

3.5. Effect of Aging Temperature on Structural Properties of CaP Powders

XRD of resultant CaP powders synthesized at 25°C and 5°C aging temperatures followed by their sintering at 300°C, 500°C, 700°C and 900°C have been shown in Figures 10-11 respectively.

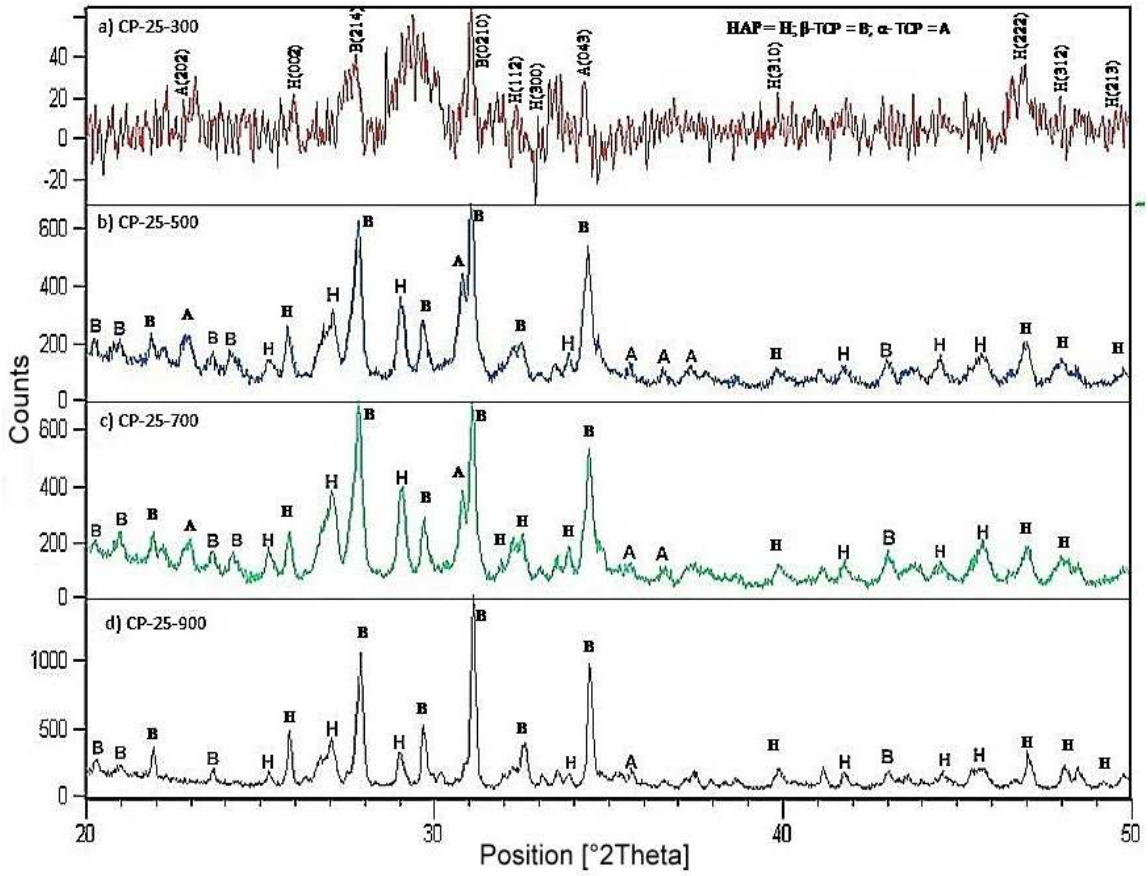

Figure 10. XRD Patterns of CaP Powders Aged at 25°C Followed by Sintering at (a) 300°C, (b) 500°C, (c) 700°C and (d) 900°C from Top to Bottom. Here CP means Calcium Phosphate

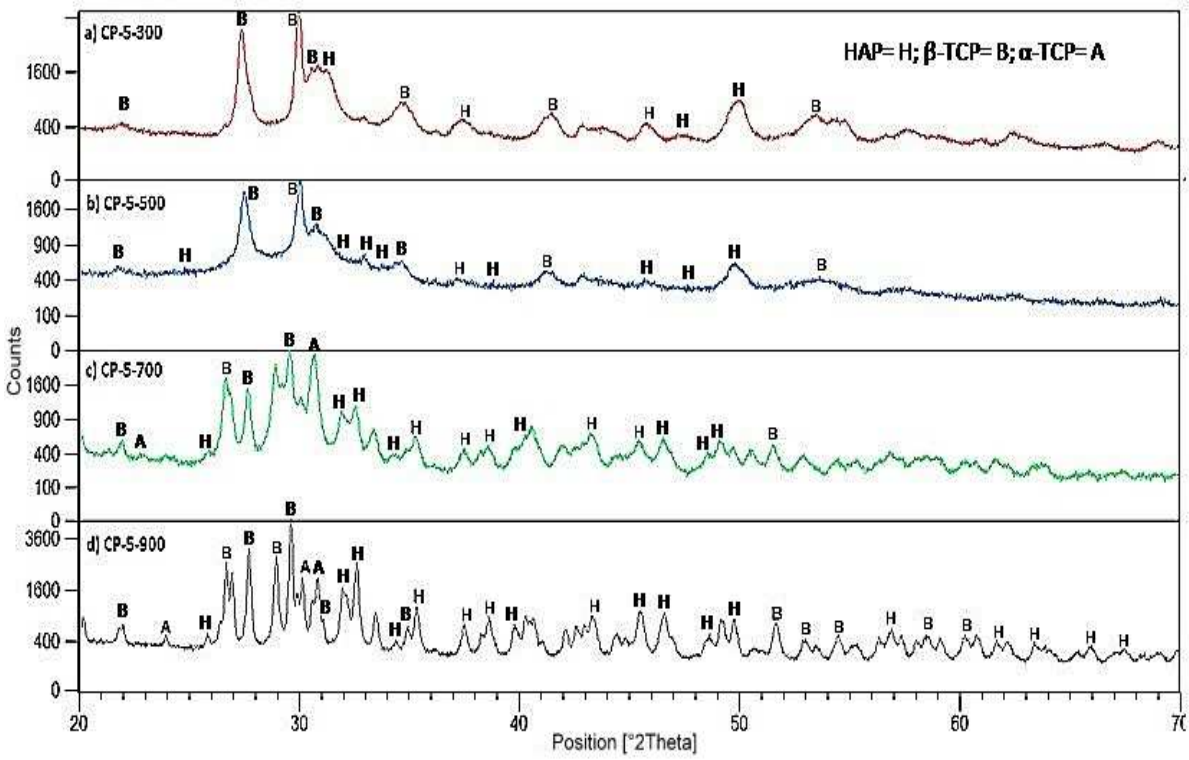

Figure 11. XRD Patterns of CaP Powders Aged at 5°C Followed by Sintering at (a) 300° C, (b) 500°C, (c) 700°C and (d) 900°C from Top to Bottom

Major phases, HAP lattice parameters, mean crystallite size, weight fractions, estimated Ca deficiency and resultant Ca/P ratio of all the powders sintered at different temperatures were categorized differently on the basis of their aging temperatures and have been briefed in Tables 1-2 respectively.

Table 1. Calculated Properties of CaP Powders Aged at 25°C

Parameters	CP-25-300	CP-25-500	CP-25-700	CP-25-900
Major Phases	HAP; β-TCP; α-TCP	HAP; β-TCP	HAP; β-TCP; α-TCP	HAP; β-TCP
HAP Lattice Parameters (nm)	a= 9.442; c= 6.859; c/a= 0.726	a= 9.313; c= 6.913; c/a= 0.742	a= 9.416; c= 6.900; c/a= 0.732	a= 9.440; c= 6.900; c/a= 0.730
Mean Crystallite Size (nm)	10.606	28.796	40.643	54.163
Weight Fractions	HAP=0.3412; β-TCP= 0.7410	HAP=0.2865; β-TCP= 0.7424	HAP=0.25; β-TCP= 0.7530	HAP=0.2720; β-TCP= 0.6968
Estimated Ca Deficiency, x	0.700	0.736	0.764	0.734
Ca/P Ratio	1.55	1.54	1.53	1.54

Table 2. Calculated Properties of CaP Powders Aged at 5°C

Parameters	CP-5-300	CP-5-500	CP-5-700	CP-5-900
Major Phases	β-TCP; HAP	β-TCP; HAP; α-TCP	β-TCP; α-TCP; HAP;	β-TCP; HAP
HAP Lattice Parameters (nm)	a= 9.503; c= 7.216; c/a= 0.759	a= 9.514; c= 6.828; c/a= 0.717	a= 9.457; c= 6.765; c/a= 0.715	a= 9.449; c= 6.593; c/a= 0.697
Mean Crystallite Size (nm)	12.965 nm	16.058 nm	65.649 nm	94.001 nm
Weight Fractions	β-TCP= 0.3727; HAP=0.3212	β-TCP= 0.3310; HAP=0.1687	β-TCP= 0.5030; HAP=0.3714	β-TCP= 0.0920; HAP=0.2948
Estimated Ca Deficiency, x	0.556	0.679	0.593	0.251
Ca/P Ratio	1.574	1.55	1.567	1.62

Peak width measurement of (0 0 2) and (3 1 0) reflections of CaP powders were used to analyze the effect of aging temperatures on their crystallinity and results have been enumerated in Tables 3-4 respectively.

Table 3. Peak Width Measurement of (0 0 2) and (3 1 0) Reflections of CaP Powder Aged at 25°C

	Planes	CP-25-300	CP-25-500	CP-25-700	CP-25-900
Peak Width (2θ)	**(002)**	0.2007	0.1004	0.2007	0.1506
	(310)	0.4015	0.2676	0.2856	0.1171

Table 4. Peak Width Measurement of (0 0 2) and (3 1 0) Reflections of CaP Powder Aged at 5°C

	Planes	CP-5-300	CP-5-500	CP-5-700	CP-5-900
Peak Width (2θ)	**(002)**	-	0.0502	0.2007	0.2007
	(310)	-	0.0612	0.2007	0.2007

Diffractograms confirmed the biphasic nature of CaP powders synthesized at both the aging temperatures primarily comprised of β-TCP and HAP in major proportions followed by α-TCP in traces. Existence of HAP at low sintering temperature of 300℃ in both the synthesized powders irrespective of aging temperatures can be considered as one of the achievement of present work owing to its suitability for coating applications having minimized oxidative degradation of underlying metal substrates [9]. Partial amorphous nature of both the CaP powders converted into crystalline powders upon increasing the sintering temperature from 300℃-500℃ as can be interpreted in terms of indistinct to distinct and clear peaks as shown in Figures 10-11 respectively. This is in accordance with the reference no.-9, which suggests that apatite having lower Ca/P ratio can be developed as amorphous complex intermediate in the gel, which then can be transformed into crystalline phases upon heating. Further observations led to the fact that no evolution of new phases take place upon sintering from 500℃-900℃ respectively irrespective of aging temperatures. Sintering temperatures increased the intensity of existing phases which is also supported by the respective TG analysis which confirm the same in terms of maximum %weight change up to the temperature of 300℃ only. This property further highlights the thermal stability of both the CaP powders beyond 500℃ respectively. Lattice distortion (c/a value) was experienced at all sintering temperatures ranging from 69-75% with HAP lattice parameters calculated to be near to reference values of a=9.418Å and c= 6.884 Å. Lattice distortion values indicate an expansion in the crystal lattice either or along both a and c axes, indicating lattice imperfection may be due to the incorporation of larger ions. This defect may be introduced as a result of higher acidity of the precursors, where more acidic phosphate HPO_4^{-2} may substitute smaller PO_4^{-3} which may, based on electrical neutrality, have a chemical form of $Ca_{10-x}(HPO_4)_x\ (PO_4)_{6-x}(OH)_{2-x}$, i.e. a calcium deficient apatite, which is agreed with Ca/P ratios as determined in present investigation. As expected, mean crystallite size increased with the rise of sintering temperature in both the synthesized powders.

Comparing the effects of aging temperature on CaP powders conclude that during aging temperature of 25℃, phase formation and thermal stability completed at a sintering temperature of 500℃, whereas the onset of similar properties started to occur at 700℃ sintering temperature in case of CaP powder prepared at an aging temperature of 5℃ respectively. Relative weight fractions of β-TCP and HAP phases were observed to be more at all sintering temperatures of CaP powder aged at 25℃ compared to one aged at 5℃. On the other hand, aging temperature of 25℃ caused the powder to be more calcium deficient than one synthesized having 5℃ aging temperature. Crystallinity of CaP powder synthesized at an aging temperature of 5°C was compared to be more than the one aged at 25℃ by comparing the peak widths of (3 1 0) planes of both the CaP powders as shown in Tables 3-4 respectively. But at a temperature of 900℃, crystallinity was observed to be more in case of powder synthesized at an aging temperature of 25℃.

Development and existence of resorbable (TCP) and bioactive (HAP) phases at all sintering temperatures may be the result of complete hydrolysis and aging of reactant precursors and their CaP sols respectively. Ironically, this TCP phase may be not an undesirable component on the basis of the biphasic calcium phosphate concept [9] recently proposed by Daculsi [37]. From practical viewpoint, it is always desirable if an implant material can be designed in such a way that it can be completely replaced by the host tissues upon a resorption-apposition mechanism. Moreover, bioresorption has been a process that is able to accelerate the growth of defective hard tissues and this mechanism implies the significant role of resorption in biological response. Therefore, non/less resorbable nature of synthetic HAP can be further modified by incorporation of more bioresorbable second phase(s). Therefore, an optimized combination of different calcium phosphates of varying degree of solubility may be a promising alternative for specific clinical purposes [9]. Based on the concept, presence of TCP phase developed in current synthesis conditions can be considered as an advantage rather than an obstacle.

3.6. Effect of Aging Temperature on Ionic Constitution of CaP Powders

Presence of various ionic groups in respective synthesized powders was confirmed by FTIR spectras and has been shown in Figures 12-13 categorized on the basis of their aging temperatures. Table 5 summarized the standard peak data and their corresponding functional groups which were used to match with the frequencies of peaks obtained in synthesized powders in the present work.

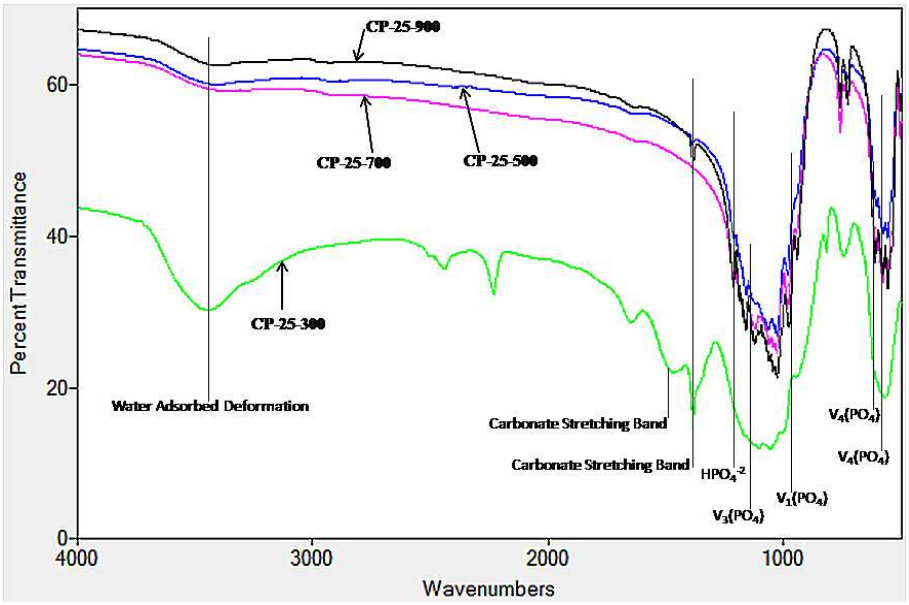

Figure 12. FTIR Spectra of Powders Aged at 25°C Followed by Sintering at 300°C, 500°C, 700°C and 900°C Temperatures

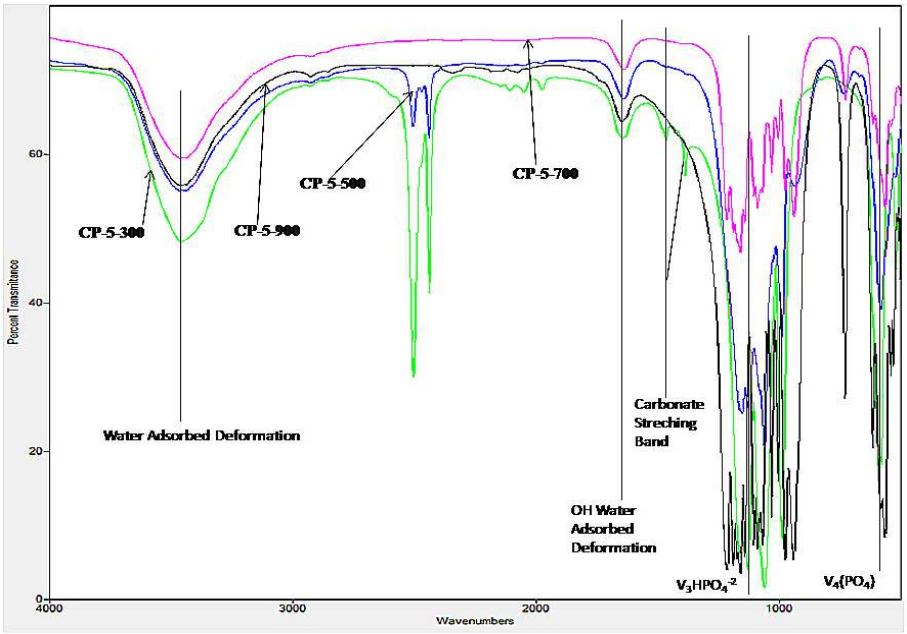

Figure 13. FTIR Spectra of Powders Aged at 5°C Followed by Sintering at 300°C, 500° C, 700°C and 900°C Temperatures

Table 5. Standard FTIR Data for HAP

Frequency cm^{-1} CDHA According to Literature[(a)]	Vibrations
3572 w	OH stretching
3400	Water-adsorbed deformation
1625	OH water adsorbed deformation
1600-1300	Carbonate stretching band
1210	δOH mode of HPO_4^{-2} hydrogen bonded
1133	ν_3 vibration component of HPO_4^{-2} gps
1087-1072 s	$\nu_3 (PO_4)$
1046-1032 vs	
962	$\nu_1 (PO_4)$
870	ν_5 P-O(H) deformation of HPO_4^{-2} gps
630 m	OH liberations
601 m	$\nu_4 (PO_4)$
571 m	
472	$\nu_2 (PO_4)$

Molecular arrangement of constituting ionic groups of powders aged and synthesized at 25℃ and 5℃ were studied by means of FTIR spectras shown in Figure 12-13 respectively. Comparison of spectras confirmed the presence of water adsorbed deformation corresponding to 3400 cm^{-1} wavenumber in both the CaP powders at all sintering temperatures. With the increase of sintering temperature, the broad band corresponding to water adsorbed deformation narrowed down in case of powder aged at 25℃, whearas it remained almost intact in case of powder aged at 5℃. In addition, OH water adsorbed deformation functional group was completely absent in case of powder aged at 25℃, whereas the same deformation was noticed and remained intact at all sintering temperatures in case of 5℃ aged powder. An atmospheric impurity i.e. carbonate ion was noticed at a sintering temperature of 300℃ corresponding to two wavenumbers of 1463.61, 1384.57 cm^{-1} in case of powder synthesized at an aging temperature of 5℃ and eloped also upon further sintering to higher temperature. On the other hand, a very sharp peak representing carbonate ion was detected at all sintering temperatures except 700℃ in case of powder aged at 25℃. It has been reported that at low temperatures, CO_3^{2-} ions might act as the role of PO_4^{3-} ions and allowed the amount of PO_4^{3-} ions to be increased, so that the Ca/P ratio decreased with the formation of the CO_3^{2-} and hence led to the occurrence of HAP/TCP biphasic carbonate-containing apatite [32]. This carbonate phosphate might come from the atmospheric carbon dioxide which combined into the crystal structure during dissolving, stirring, reaction and calcining process [10]. It is similar to the natural bone mineral because bone mineral differs in composition from stoichiometric HAP in which carbonate is the most abundant additional ions [10]. In addition, carbonate containing and calcium deficient HAP is more thermodynamically favored than stoichiometric HAP [28]. Third vibrational mode of HPO_4^{-2} ionic species was also detected in the powders synthesized at both the aging temperatures of 25℃ and 5℃ throughout respectively. Number of vibrational groups corresponding to PO_4^{-2} ion increased with the increase of sintering temperature at both the aging temperatures.

Quantitatively, more PO_4^{-2} ionic groups were detected in powder aged at 25℃ as compared to one aged at 5℃, whereas lesser number of HAP inhibiting impurities such as carbonate and hydrogen phosphate was detected in powder aged at 5℃ than the other, qualitatively. Presence of carbonate ions at all sintering temperatures confirms the more thermodynamically stable nature of CaP powder aged at 25℃ than the one aged at 5℃ respectively. Presence of PO_4^{-2} ions right from 300℃ sintering using FTIR results further supports the XRD results and confirms the existence of HAP phase throughout all sintering temperatures, which is one of the achievement of the present work of HAP formation at low temperatures using sol-gel technique. Lesser number of impurities as detected by FTIR study further supports the XRD results of having better Ca/P ratio in powder aged at 5℃. Thus FTIR analysis justifies the XRD results of calcium deficient biphasic nature of powders and also enumerated the reason of presence of allied impurities in the formula of resultant constituting compounds.

3.7. Effect of Aging Temperature on Thermal Properties of CaP Powders

Thermal behavior of gels aged at 25℃ and 5℃ was ascertained and recorded using Thermogravimetric-cum-Differential Scanning Calorimetry (TG/DSC) technique. Corresponding results have been shown in Figures 14-15 differentiated on the basis of their aging temperatures.

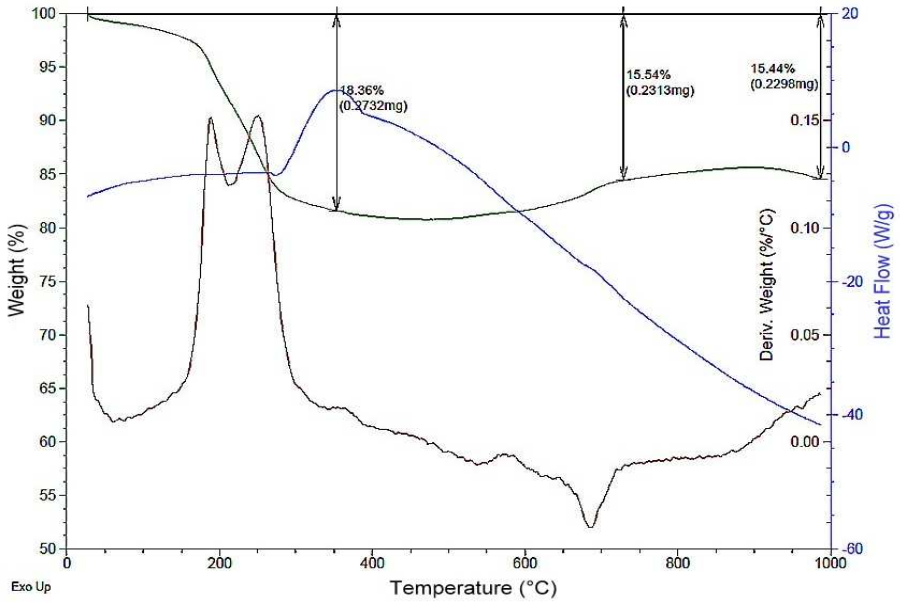

Figure 14. Combined TG/DSC Thermogram of Gel Aged at 25°C

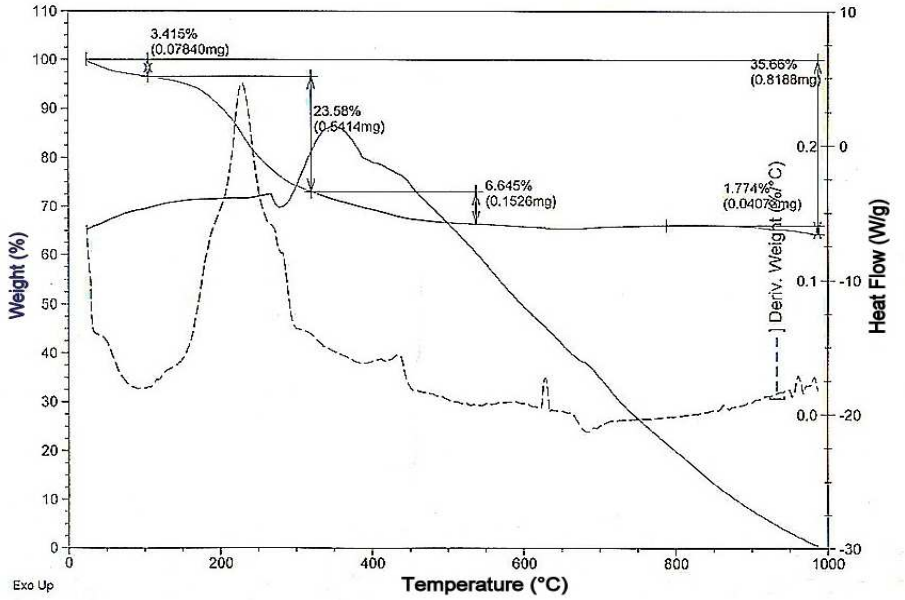

Figure 15. Combined TG/DSC Thermogram of Gel Aged at 5°C

Comparison of TG plots as shown in Figures 14-15 indicates of more weight loss of 35.66% in case of gel prepared at an aging temperature of 5℃, whereas maximum of 18.36% of weight loss was observed in case of aging temperature of 25℃ which is approximately half of the former weight loss. Maximum weight loss occurred up to the sintering temperature of 300℃ in both the gels. Large exothermic peaks before 300℃ in both the aged gels may be primarily due to the removal of adsorbed water and free solvents i.e. most probably C_2H_5OH which caused the weight to decrease rapidly.

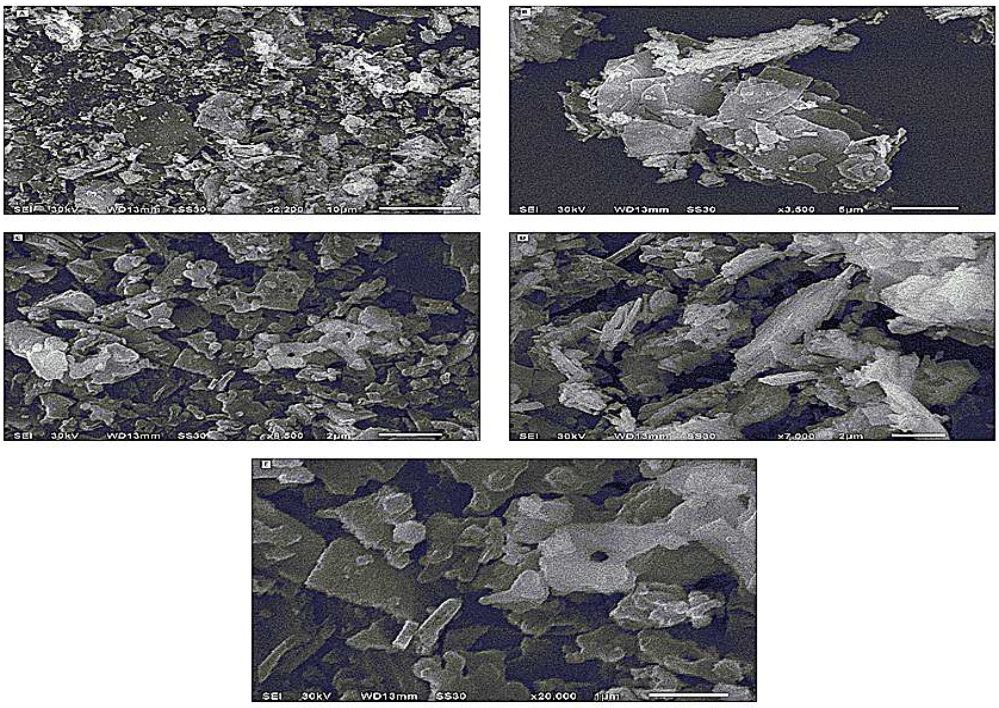

Figure 16. SEM Micrographs of Powder Aged at 25°C and Sintered at 900°C at Various Magnifications

From 300℃-500℃, weight loss was negligible in case of gel aged at 25℃, whereas it was noted to be 6.645% in case of 5℃ aged gel. Interestingly and strangely, onset of weight gain was observed on further heating to 700℃ (15.54%) and 900℃ (15.44%) in case of gel prepared at an aging temperature of 25℃ as shown in Figure 14. This weight gain may be attributed to the inclusion of carbonate ions into molecular structure of CaP gel aged at 25℃ as also indicated by FTIR analysis. Therefore, comparing the %weight losses, CaP gel prepared at 25℃ aging

temperature has been concluded to be more (approximately 02 times) thermodynamically stable in lines with XRD and FTIR analysis.

3.8. Effect of Aging Temperature on Morphological and Elemental Properties of CaP Powders

After comprehensive structural analysis of synthesized powders; morphology, shape, size and spread of powder particles prepared at 25°C and 5°C aging temperatures followed by sintering at 900°C only were verified using Scanning Electron Microscopy (SEM) and respective micrographs have been shown in Figures 16-17 respectively.

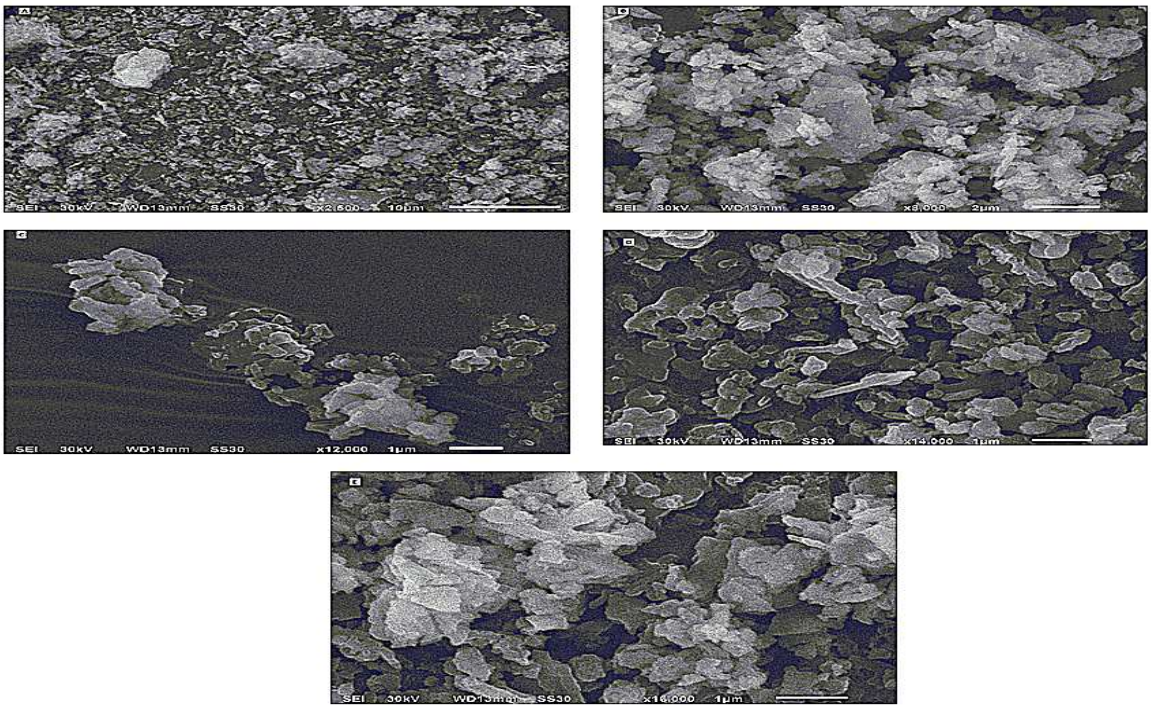

Figure 17. SEM Micrographs of Powder Aged at 5°C and Sintered at 900°C at Various Magnifications

Presence of various constituting elements in powders was also detected using Energy Dispersive (EDX) spectroscopy. Micrographs and corresponding elements have been shown in Figures 18-19 differentiated on the basis of aging temperatures respectively.

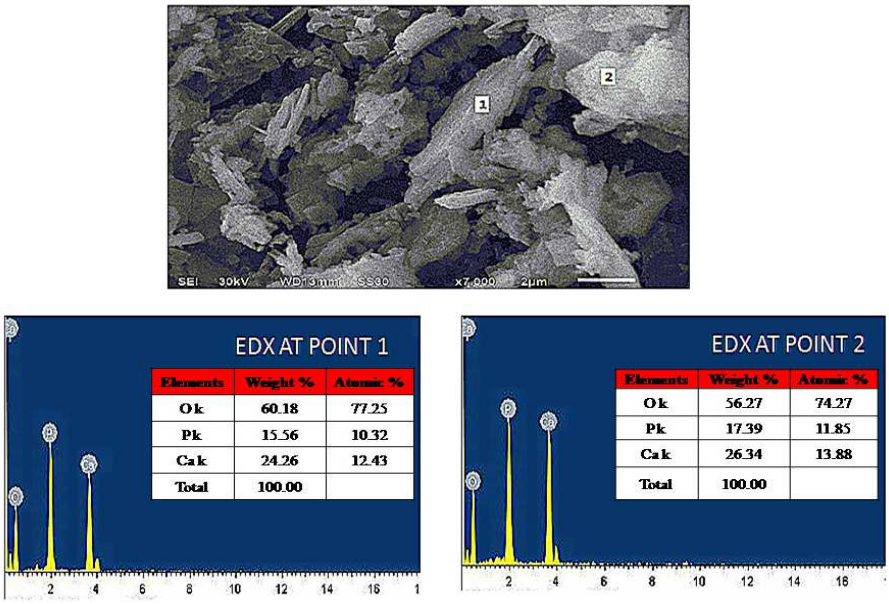

Figure 18. SEM & EDX Micrographs of Powder Aged at 25°C and Sintered at 900°C

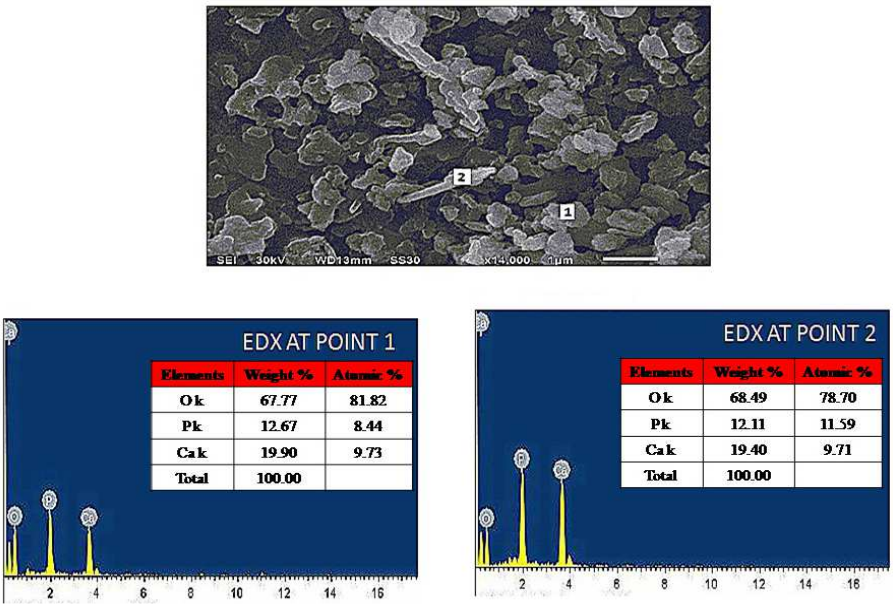

Figure 19. SEM & EDX Micrographs of Powder Aged at 5° C and Sintered at 900° C

Granular, irregular, smooth, loose, non-agglomerated particles primarily of solid and plate like shapes having wide range of sizes were detected for powder aged at 25°C temperature. Similarly, powder prepared at an aging temperature of 5°C was also comprised of little agglomerated granular, irregular particles of nano-dimensional structure having vivid particle sizes of rod and plate like shapes. Average particle size ranges from 100-150 µm with an aspect ratio of 1.531 and mean roundness of 0.779 were the properties of powder synthesized at an aging temperature of 25°C. On the other hand, a little larger particles ranging from 105-185 µm with an aspect ratio of 1.552 and mean roundness of 0.767 were measured in case of powder aged at 5°C. Grain boundaries were visible in both the structures, but only at higher magnifications.

As expected, EDX analysis clearly showed the presence of O, Ca and P in varied weight% in both the synthesized powders aged at 25°C and 5°C respectively, thus validating the phase analysis predicted by XRD. Ca/P ratio detected by EDX was calculated to range between 1.51-1.55 and 1.57-1.60 for CaP powders aged at 25°C and 5°C respectively which is close enough as predicted by XRD.

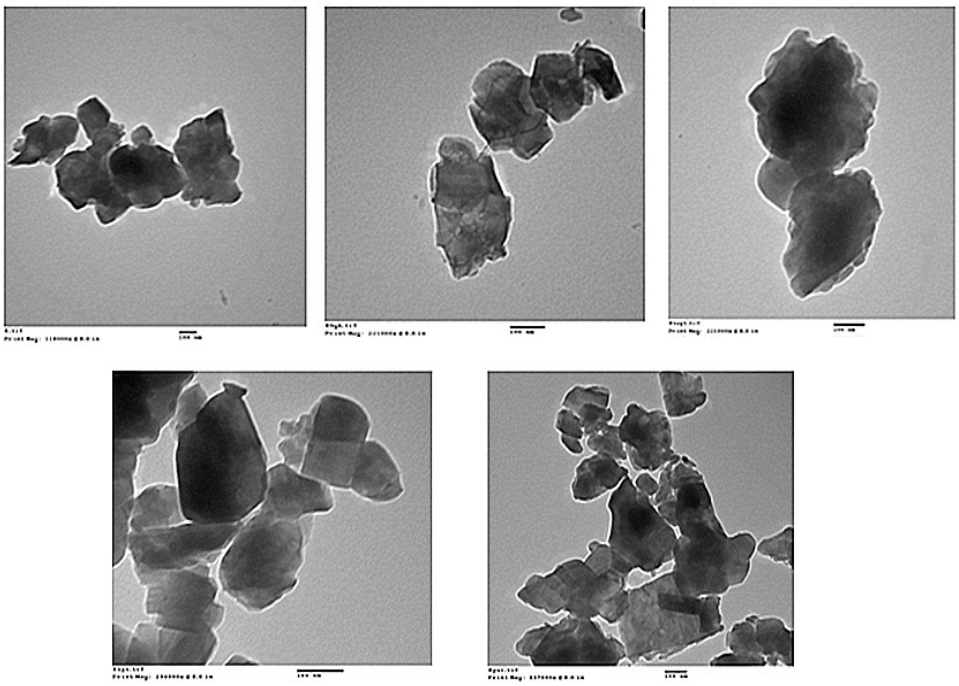

Figure 20. Nanographs of Powder Aged at 25°C and Sintered at 900°C at Various Magnifications

3.9. Effect of Aging Temperature on Crystal Structure of CaP Powders

Crystal size and shape of CaP powders were characterized using Transmission Electron Microscopy (TEM) technique. Nanographs of powders aged and synthesized at 25° C and 5℃ have been shown in Figures 20-21 respectively revealing their approximate hexagonal shape and corresponding sizes.

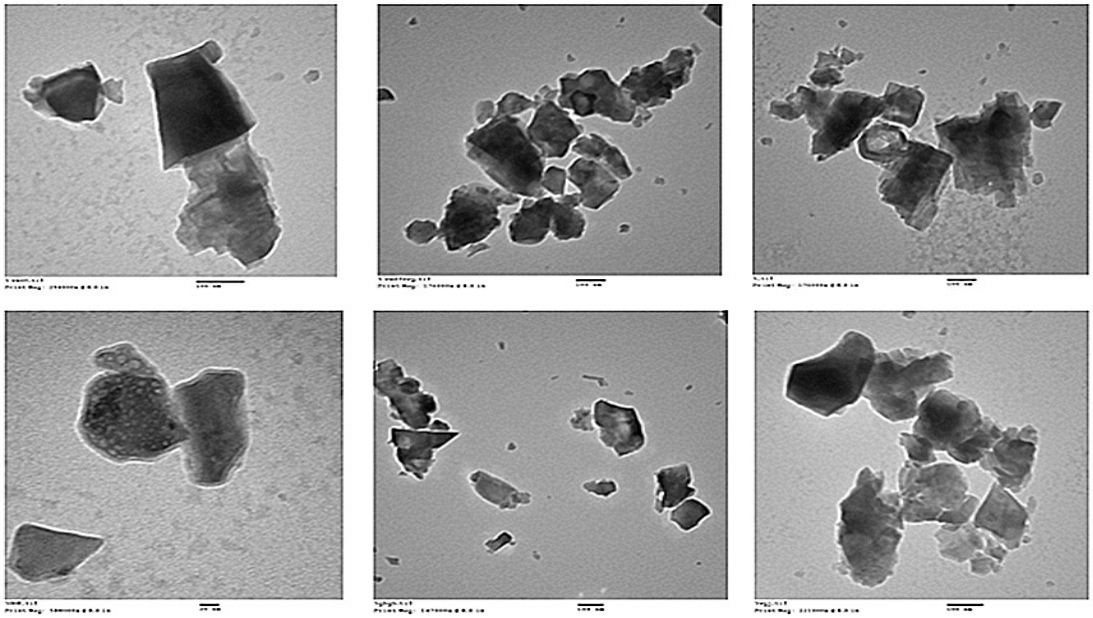

Figure 21. Nanographs of Powder Aged at 5°C and Sintered at 900°C at Various Magnifications

TEM analysis was carried out on fully crystalline powders sintered at 900℃. Figures 20-21 characterized the nearly hexagonal shape of crystals having sharp edges and corners irrespective of difference of aging temperatures. Average crystal size was measured to range between 102-23 nm having aspect ratio and roundness of 1.528 and 0.789 in case of 25℃ aged CaP powder, whereas smaller crystals of 95-189 nm having approximately similar aspect ratio and roundness of 1.629 and 0.759 were measured in 5℃ aged powders.

CONCLUSION

Complete hydrolysis of CNT and TEP precursors produced encouraging results viz. constant pH of CaP sols, rapid and stable phase formation, thermal stability from lower temperatures onwards and HAP formation at lower sintering temperatures etc. Higher aging temperature of 25℃ produced more weight fractions of β-TCP and HAP phases, having carbonated ions in molecular structure providing higher thermal stability to synthesized CaP powders than the one prepared at an aging temperature of 5℃ respectively. Furthermore, aging temperature was also found to affect the particle and crystal shape and sizes. Larger, non-agglomerated, hexagonal crystals having nanoregime were synthesized. This investigation concluded that the higher aging temperature of 25℃ to be optimum having all desirable properties as required for any biocompatible bioceramic suitable to be used in the human bodies.

REFERENCES

[1] LL Hench. *Journal of the American Ceramic Society*, **1998**, 81, 1705–1728.
[2] SJ Kalita; HA Bhatt. *Materials Science and Engineering*, **2007**, 27, 837-848.
[3] S Dorozhkin; M Epple. *Angewandte Chemie International Edition*, **2002**, 41, 3130-3146.
[4] SH Kwon; HK Jun; SH Hong; HE Kim. *Journal of European Ceramic Society*, **2003**, 23, 1039-1045.
[5] J Chen; Y Wang; X Chen; Li Ren; C Lai; W He; Q Zhang. *Materials Letter*, **2011,** 65, 1923-1926.
[6] TK Anee; M Ashok; M Palanichamy; S Narayana Kalkura. *Materials Chemistry and Physics*, **2003**, 80, 725-730.
[7] DM Liu; Q Yang; T Troczynski; WJ Tseng. *Biomaterials*, **2002,** 23, 679-1687.
[8] CS Chai; KA Gross; BB Nissan. *Biomaterials*, **1998**, 19, 2291-2296.
[9] DM Liu; T Troczynski; D Hakimi. *Journal of Materials Science: Materials in Medicine,* **2002**, 13, 657-665.
[10] J Chen; Y Wang; X Chen; Li Ren; C Lai; W He; Q Zhang. *Materials Letter*, **2011**, 65, 1923-1926.
[11] RR Rao; HN Roopa; TS Kannan. *Journal of Material Science: Materials in Medicine*, **1997**, 8, 511-518.
[12] HK Varma; SN Kalkura; R Sivakumar. *Ceramic International*, **1998**, 24, 467-470.
[13] S Sarig; F Kahana. *Journal of Crystal Growth*, **2002**, 237-239, 1, 55-59.

[14] GK Lim; J Wang; CH Chew; LM Gan. *Biomaterials*, **1997**, 18(21), 1433-1439.
[15] C Duan; J Wang; S Zhou; B Feng; X Lu and J Weng. *Journal of Sol-Gel Technology*, **2012** 63, 126-134.
[16] J Dong; T Uemura; Y Shirasaki; T Tateishi. *Biomaterials*, **2002**, 23, 4493–4502.
[17] P Layrolle; A Ito; T Tateishi. *Journal of American Ceramic Society*, **1998**, 81, 1421-1428.
[18] A Jillavenkatesa; RA Condrate. *Journal of Material Science*, **1998**, 33, 4111-4119.
[19] CM Lopatin; V Pizziconi; TL Alford; T Laursen. *Thin Solid Films*, **1998**, 326, 227-232.
[20] X Liu; PK Chu; C Ding. *Material Science and Engineering R*, **2004**, 47, 49-121.
[21] LD Piveteau, in: DM Brunette; P Tengvall; M Textor; P Thompson (Eds.), Titanium in Medicine, Springer, Berlin, **2001**, 267-282.
[22] BB Nissan; DD Green; GSK Kannangara; CS Chai; A Milev. *Journal of Sol-Gel Science and Technology*, **2001**, 21, 27-37.
[23] MF Hsieh; LH Perng; TS Chin; HG Perng. *Biomaterials*, **2001**, 22, 2601-2607.
[24] Y Masuda; K Matubaram; S Sakka. *Journal of Ceramic Society of Japan*, **1990**, 98, 1266.
[25] F Azem; A Cakir. *Journal of Sol-Gel Science and Technology*, **2009,** 51, 190-197.
[26] U Vijayalakshmi; S Rajeswari. *Journal of Sol-Gel Technology*, **2012,** 63, 45-55.
[27] KA Gross; CS Chai; GSK Kannangara; BB Nissan. *Journal of Materials Science: Materials in Medicine*, **1998**, 9, 839-843.
[28] SR Paital; NB Dahotre. *Acta Biomaterialia*, **2009**, 5, 2763-2772.
[29] DM Liu; T Troczynski; WJ Tseng. *Biomaterials*, **2002**, 23(4), 1227-1236.
[30] C You; S Oh; S Kim. *Journal of Sol-Gel Science and Technology*, **2001**, 21, 49-54.
[31] HM Kim; F Miyaji; T Kokubo. *Journal of Materials Science: Materials in Medicine*, **1997**, 8, 341-347.
[32] C Duan; J Wang; S Zhou; B Feng; X Lu; J Weng. *Journal of Sol-Gel Science and Technology*, **2012**, 63, 126-134.
[33] Y Masuda; K Matbara; S Sakha. *Journal of Ceramic Society Japan*, **1990**, 98, 1266-1277.
[34] FH Westheimer; S Huang; F Coritz. *Journal of American Chemistry Society*, **1988**, 110, 181-185.
[35] J Livage; P Barboax; MT Vandenborre; C Sichmutz; F Taulflle. *Journal of Non-Crystalline Solids*, **1992**, 147/148, 18-22.
[36] J Livage; M Henry; C Samchez. *Progress in Solid State Chemistry*, **1988**, **18**, 259-341.
[37] G Daculsi. *Biomaterials*, **1998**, 19, 1473-1478.